

The site of action potential initiation in cerebellar Purkinje neurons

Beverley A Clark^{1,3}, Pablo Monsivais^{1,3}, Tiago Branco², Michael London¹ & Michael Häusser¹

Knowledge of the site of action potential initiation is essential for understanding how synaptic input is converted into neuronal output. Previous studies have shown that the lowest-threshold site for initiation of action potentials is in the axon. Here we use recordings from visualized rat cerebellar Purkinje cell axons to localize the site of initiation to a well-defined anatomical structure: the first node of Ranvier, which normally forms at the first axonal branch point.

Although recordings from the axon initial segment in various neuronal types have demonstrated that action potential initiation normally occurs in the axon^{1–5}, the precise site of action potential initiation within the axon remains unknown. This is in part due to the difficulty of making direct axonal recordings at substantial distances from the

soma. To facilitate axonal recordings, we filled rat cerebellar Purkinje neurons with a fluorescent dye and imaged the axons using a CCD camera (Fig. 1a and Supplementary Methods online; all procedures were carried out according to U.K. Home Office regulations). This permitted cell-attached patch-clamp recordings to be made from the axon under direct visual control.

To identify the site of action potential initiation in the axon, we made simultaneous multiple patch-clamp recordings of extracellular action currents from the soma and from locations at various distances down the axon (Fig. 1a–c) during spontaneous firing of Purkinje cells, which occurs at rates comparable to those found *in vivo*⁶. Previous studies have shown that action potentials in the initial segment of the axon precede those recorded at the soma^{1,2,4,5}. We predicted that this negative time difference between the axonal and the somatic action potential should be greatest at the site of initiation of the action potential. Figure 1d shows that there is a V-shaped relationship between the axonal-somatic action potential latency and the distance of the axonal recording site. The site of initiation of the action potential was identified as the nadir of this relationship, corresponding to the largest axon-soma latency advance. This occurred at a distance of $75 \pm 11 \mu\text{m}$ from the soma (measured from a bilinear fit to the data points; $n = 68$ recordings). The latencies were very similar for spontaneous action potentials recorded in cell-attached recordings and those evoked by depolarizing current pulses in somatic

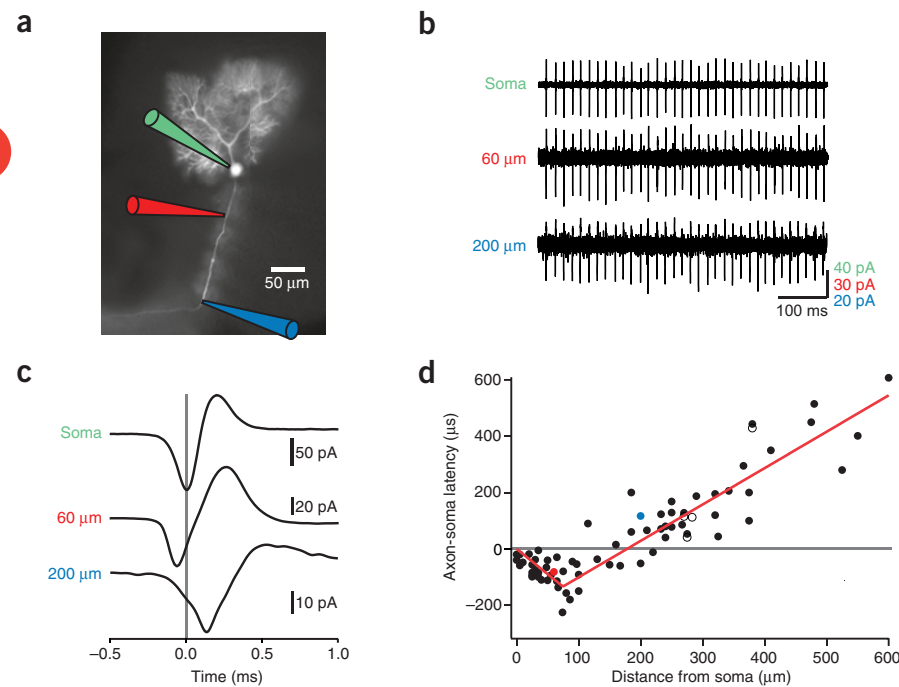


Figure 1 Direct measurement of the initiation site during spontaneous action potential firing. (a) Fluorescence image of a Purkinje cell filled with Alexa 488, illustrating the recording configuration. (b) Simultaneous triple cell-attached recording of spontaneous action potentials from the soma (top electrode) and at two locations along the axon (middle and bottom electrodes, 60 and 200 μm) of the same Purkinje neuron shown in a. (c) Latency differences between the somatic action potential (aligned to $t = 0$ at its first peak) and the action potential at the two axonal recording sites (averages of 50 action potentials are shown). (d) Latency differences of spontaneous action potentials for 68 simultaneous somatic and axonal recordings (colored data points correspond to the recording in c; open circles are latencies from the derivatives of somatic whole-cell voltage recordings where action potentials were evoked using 0.1–0.3 nA current pulses). A bilinear fit to the data is shown, giving a maximum axon-soma advance at $75 \pm 11 \mu\text{m}$; its slope indicates antidiromic and orthodromic axonal propagation velocities of 0.56 ± 0.11 and $0.77 \pm 0.05 \text{ m s}^{-1}$, respectively.

¹Wolfson Institute for Biomedical Research, Department of Physiology, and ²MRC Laboratory for Molecular Cell Biology, University College London, Gower Street, London WC1E 6BT, UK. ³These authors contributed equally to this study. Correspondence should be addressed to M.H. (m.hausser@ucl.ac.uk).

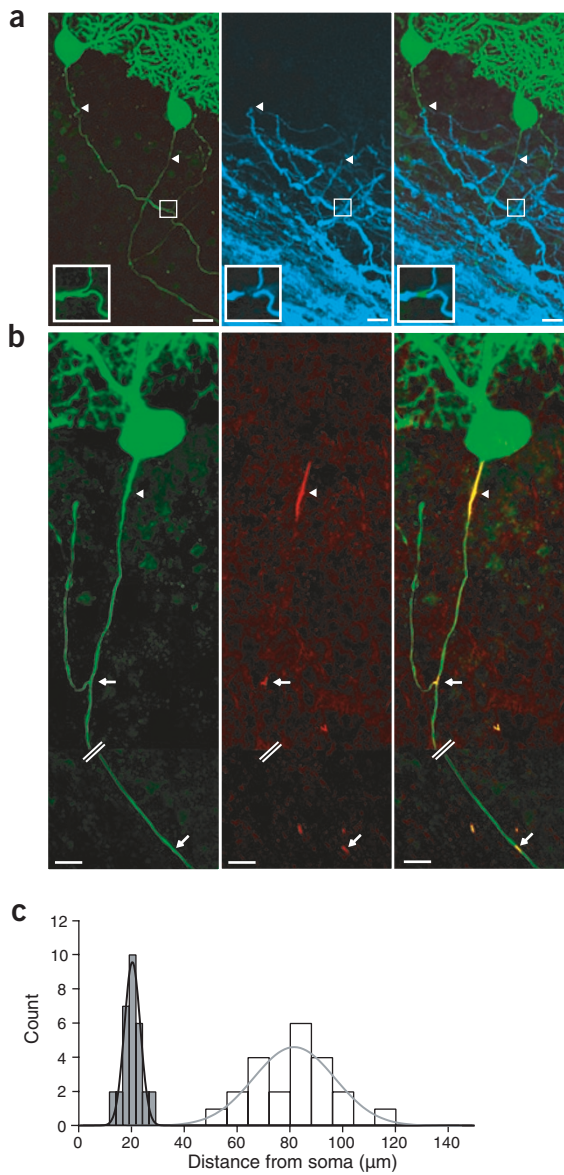


Figure 2 The action potential initiation site corresponds to the first branch point. **(a)** Confocal images of Purkinje cells filled with biocytin (green, left) and counterstained against MBP (blue, middle) to show the myelin and its relationship to the individual Purkinje cells (overlay, right). Arrowheads point to the starting point of the myelin (and thus the end of the initial segment). The inset shows the first node/branch point (MBP stain not in the plane of the labeled axon digitally removed for clarity). Scale bar: 15 μm for main image, 5 μm for inset. **(b)** Confocal images of Purkinje cells filled with biocytin (green, left) and counterstained against ankyrin-G (red, middle). The arrowhead indicates the initial segment, the top arrow the first node and the lower arrow the second node (lower panel; 312 μm from the soma; intervening axon cut). Scale bar: 10 μm. **(c)** Histogram showing distance to the end of the initial segment (gray bars: 2 μm bins) and the first branch point (white bars: 8 μm bins) measured from the point of origin of the axon from the soma. Gaussian fits to the data points are shown. Mean values were $21 \pm 4 \mu\text{m}$ ($n = 31$) and $82 \pm 14 \mu\text{m}$ ($n = 22$) from the soma, respectively.

which links voltage-gated Na^+ channels to the cytoskeleton and is closely associated with axonal Na^+ channels in many neuronal types⁸. Dense ankyrin-G immunofluorescence was detected at axon initial segments⁸ and at the first node of Ranvier, highlighting the Y-shaped bifurcation of the branch point (Fig. 2b). Ankyrin-G immunofluorescence also allowed reliable identification of the second node, which was located $346 \pm 30 \mu\text{m}$ from the soma ($n = 3$; Fig. 2b), thus ruling out the second node as the site of initiation. Taken together, these findings indicate that the site of origin of the action potential corresponds to the first node, which is normally at the first axonal branch point.

To investigate the geometric constraints on spike initiation in Purkinje cell axons, we designed a computer model based on the morphology of a Purkinje cell (Fig. 3 and Supplementary Videos 1 and 2 online), incorporating a detailed reconstruction of its axon. The model successfully reproduced our experimental data on action potential initiation, and demonstrated that during action potential initiation, the spatial spread of the membrane potential initially showed a single sharp maximum at the first node and then fell steeply, attenuating by more than two-thirds of its amplitude at the initial segment or second node. Indeed, such a spatial profile was required to produce latency differences that matched our experimental data. The model thus confirms that initiation does occur at a specific location, namely the first node of Ranvier, and therefore serves as an important ‘proof of concept’ supporting our experimental conclusions.

We have provided the first direct localization of the site of initiation of action potentials in a mammalian CNS neuron. The correspondence of the initiation site with the first node resolves a longstanding controversy: both early work in motoneurons⁹ and more recent studies in Purkinje cells² and pyramidal cells^{4,5,10} were unable to definitively resolve whether the action potential is initiated at the distal end of the initial segment, the first or second nodes or even further down the axon. It will be of great interest to explore how axonal geometry, channel properties and densities interact to target initiation to the first node, and whether similar rules hold in other neuronal types. The location of the initiation site at the first node may reflect a balancing of conflicting requirements. The initiation site should be at some distance from the soma, both to minimize the effect of dendritic capacitance on threshold^{10,11} and to reduce the impact of the large axonal action potential conductances on synaptic integration¹². This provides the most efficient use of the available Na^+ channels, with the initial section of myelin further minimizing the effective capacitance ‘visible’ to the node, thus reducing the number of Na^+ channels required for spike initiation and the energetic demands on the neuron associated with action potential firing¹³. However, if the action potential is initiated too far down the axon, this weakens the strength and precision of the link between synaptic input

whole-cell recordings (Fig. 1d), and they were not affected by SR95531 (10 μM), an antagonist of inhibitory synaptic transmission ($n = 4$; $P = 0.4$). Increasing the action potential frequency to 180–200 Hz to match high-frequency firing rates observed *in vivo*⁶ also did not change the latency as compared to spontaneous firing ($n = 9$; $P = 0.14$).

Does the physiologically determined site of action potential initiation correspond to a particular anatomical feature of the axon? To address this question, we examined the structure of the axon using confocal microscopy of fluorescently labeled Purkinje cells in the same preparation (see Supplementary Methods online). The physiological initiation site corresponded very well with the origin of the first axonal branch point, giving rise to an axonal collateral measured to be $82 \pm 14 \mu\text{m}$ from the soma ($n = 22$; Fig. 2; ref. 7). To determine the relationship between the branch point and myelination, we stained for myelin using immunofluorescent labeling of myelin basic protein (MBP). This showed that the initial segment terminated at only $21 \pm 4 \mu\text{m}$ from the soma (Fig. 2; $n = 31$), ruling out the initial segment as the site of initiation. Furthermore, the first node of Ranvier was observed to occur at the first branch point (Fig. 2c; $n = 22$ of 22 axons). We confirmed and extended these observations using immunofluorescent labeling of ankyrin-G,

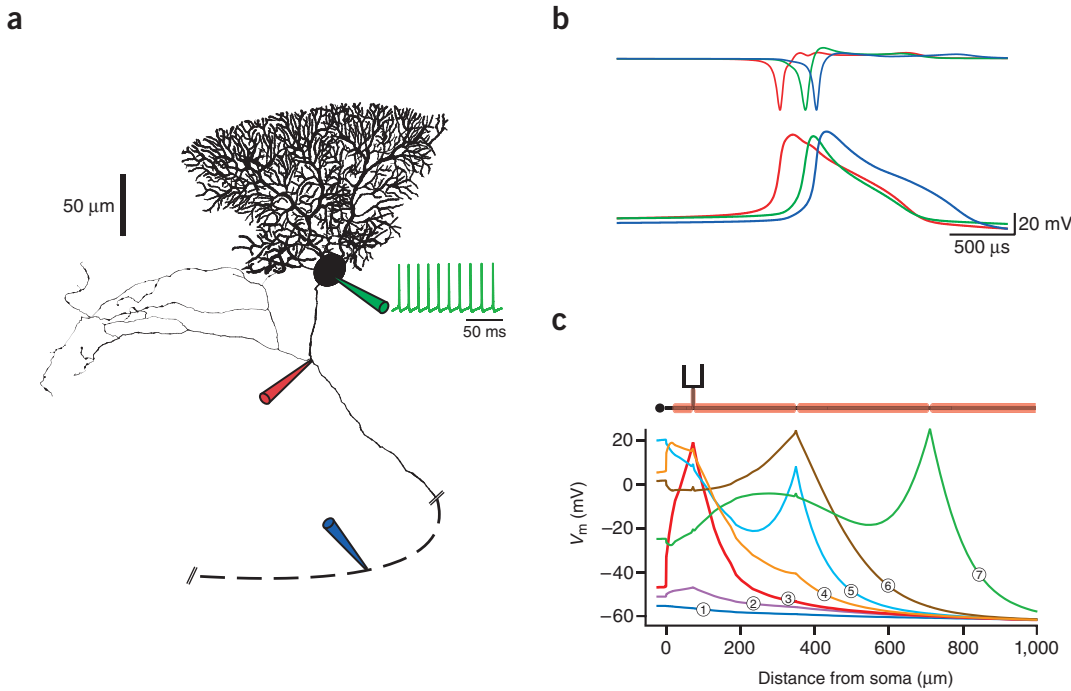


Figure 3 A model of action potential initiation in Purkinje neurons. (a) Reconstructed Purkinje neuron used for the model. The axon was extended artificially (dashed line; see **Supplementary Methods**). The inset shows spontaneous action potential firing in the model. (b) Capacitive currents (upper traces, inverted and normalized) and voltage traces of the action potential at the first node of Ranvier (red), soma (green) and the second node of Ranvier (blue). The latency difference between the peaks of the downward currents at the first node and the soma was 195 μs, consistent with our experimental data (Fig. 1d). (c) A schematic diagram of the axon, indicating the relative locations of nodes of Ranvier (top). The graph shows the voltage profile along the length of the axon at different time points during action potential initiation: 11.295 ms (1), 16.245 ms (2), 16.485 ms (3), 16.645 ms (4), 16.730 ms (5), 16.845 ms (6) and 17.145 ms (7) after the peak of the previous action potential.

and spike output, and propagation to the soma may be less secure and associated with significant delays. The targeting of inhibitory input onto the axon initial segment¹⁴, exemplified by the ‘pinceau’ arrangement of basket cell axon terminals on Purkinje cells¹⁵, could be an additional constraint such that the location of the initiation site at the first node may afford some protection from asynchronous inhibitory synaptic conductances. Understanding how these different constraints are balanced to result in the localization of the initiation site should provide fundamental insights into the regulation of neuronal excitability.

Note: Supplementary information is available on the Nature Neuroscience website.

ACKNOWLEDGMENTS

We thank J. T. Davie, J.J.B. Jack, C. Racca and A. Roth for helpful comments; V. Bennett for the ankyrin-G antibody; and A. Gidon, L. Ramakrishnan, E. Rancz, and A. Roth for help with reconstructions and videos. This work was supported by grants from the Wellcome Trust, European Commission, and the Gatsby Foundation. M.L. is a Long-Term Fellow of the Human Frontier Science Program, and T.B. was funded by the Wellcome Trust 4-year PhD Programme in Neuroscience.

COMPETING INTERESTS STATEMENT

The authors declare that they have no competing financial interests.

Received 13 October; accepted 20 December 2004

Published online at <http://www.nature.com/natureneuroscience/>

1. Stuart, G.J. & Sakmann, B. *Nature* **367**, 69–72 (1994).
2. Stuart, G. & Häusser, M. *Neuron* **13**, 703–712 (1994).
3. Häusser, M., Stuart, G., Racca, C. & Sakmann, B. *Neuron* **15**, 637–647 (1995).
4. Colbert, C.M. & Johnston, D. *J. Neurosci.* **16**, 6676–6686 (1996).
5. Stuart, G., Schiller, J. & Sakmann, B. *J. Physiol. (Lond.)* **505**, 617–632 (1997).
6. Armstrong, D.M. & Rawson, J.A. *J. Physiol. (Lond.)* **289**, 425–448 (1979).
7. Gianola, S., Savio, T., Schwab, M.E. & Rossi, F. *J. Neurosci.* **23**, 4613–4624 (2003).
8. Zhou, D. *et al.* *J. Cell Biol.* **143**, 1295–1304 (1998).
9. Coombs, J.S., Curtis, D.R. & Eccles, J.C. *J. Physiol. (Lond.)* **139**, 232–249 (1957).
10. Colbert, C.M. & Pan, E. *Nat. Neurosci.* **5**, 533–538 (2002).
11. Mainen, Z.F., Joerges, J., Huguenard, J.R. & Sejnowski, T.J. *Neuron* **15**, 1427–1439 (1995).
12. Häusser, M., Major, G. & Stuart, G.J. *Science* **291**, 138–141 (2001).
13. Attwell, D. & Laughlin, S.B. *J. Cereb. Blood Flow Metab.* **21**, 1133–1145 (2001).
14. Somogyi, P., Tamás, G., Luján, R. & Buhl, E.H. *Brain Res. Brain Res. Rev.* **26**, 113–135 (1998).
15. Eccles, J.C., Ito, M. & Szentágothai, J. *The Cerebellum as a Neuronal Machine* (Springer-Verlag, Berlin, 1967).